RESEARCH ARTICLE

**Editorial Process:** Submission:16/12/2025 Acceptance:17/08/2026 Published:26/08/2026

# Influence of Exosomes on Tumorigenic Behavior in Triple-Negative Breast Cancer Cells through *STAT3* Inhibition in Autophagy

**Shymaa Abdullah Mohamed[1]*, Mohamed Ahmed Abdel Mohsen[2], Fatma El-Zahraa A. Omar[2], Toka Mohamed Ibrahim Badawy[2], Mohammed Salama[3], Yasser Moustafa El Kerm[4], Amr Mohamed Hussein[5]**

## Abstract

**Objectives:** The prime aim of this research was to evaluate the effect of exosomes on the tumorigenic behavior of TNBC via the autophagic process. **Materials and Methods:** TNBC cell lines, MDA-MB-231 and HCC1806 cells, and non-TNBC cell line, MCF-7 cells, were utilized in this study. Cells were maintained in the presence of isolated exosomes, after characterization, before and after the downregulation of the *STAT3* signaling pathway. The cell cycle and apoptosis were analyzed using flow cytometry. Moreover, to evaluate overall autophagic flux, LC3B levels were measured by ELISA, and the expression of autophagy-related genes, *Beclin-1, ATG16L, ATG5*, and *RAB24*, was analyzed using qRT-PCR. **Results:** The results of this study may suggest that TNBC-derived exosomes play a central role in the tumorigenic behavior of breast cancer by manipulating the autophagic machinery. **Conclusion:** Accordingly, it may be concluded that the potentiation of the aggressive behavior of TNBC cells by exosomes could be autophagy-dependent, while that in NTNBC cells is autophagy-independent.

**Keywords:** Exosomes, Triple negative breast cancer, *STAT3* signaling pathway, Autophagy, Apoptosis/cell cycle

*Asian Pac J Cancer Prev,* **27 (8)**, 2909-2921

## Introduction

Triple-negative breast cancer (TNBC) is a specific subtype of breast cancer characterized by the lack of expression of *ER, PR*, and *HER2*. As a result, the growth of TNBC cells is not driven by *ER, PR*, or *HER2*. Perhaps TNBC does not respond to endocrine therapies or *HER2*-targeted agents [1]. It constitutes approximately 10-20% of all breast cancers [2] and typically exhibits a more aggressive clinical behavior compared to other breast cancer subtypes, with a higher likelihood of early metastasis and disease recurrence following treatment. It frequently presents at a higher histological grade and often displays basal-like cellular morphology [1].

Autophagy represents a fundamental cellular mechanism responsible for the transport of diverse intracellular cargo to lysosomes for degradation and recycling. In cancer, however, autophagy exhibits dual and seemingly paradoxical roles, functioning in tumor suppression during early oncogenesis while supporting survival, metabolic adaptation, and progression in established and metastatic tumors. However, in breast cancer, autophagy may play a crucial role in tumor progression, although the mechanism by which autophagy regulates metastatic potential is still unclear [3]. Type II programmed cell death in cancer cells is controlled by a network of intricate signaling pathways, such as the signal transducer and activator of transcription 3 (*STAT3*) signaling. This crosstalk between autophagy and these signaling pathways may determine the fate of cell survival or death [4]. The pivotal role of *STAT3* has been widely recognized as a regulator of gene expression related to the tumorigenic behavior of breast cancer, especially TNBC, and the regulation of several types of processes, including autophagy. *STAT3* not only induces the expression of cancer-related genes but also interacts with and collaborates with other oncogenic transcription factors, enhancing the aggressiveness of TNBC [5, 6].

Exosomes are extracellular vesicles, typically 30-150 nm in diameter, secreted by the majority of eukaryotic cells

*[1]Molecular Biology Unit, Medical Technology Center & Applied Medical Chemistry Department, Medical Research Institute, Alexandria University, Alexandria, Egypt. [2]Applied Medical Chemistry Department, Medical Research Institute, Alexandria University, Alexandria, Egypt. [3]Department of Histochemistry and Cell Biology, Medical Research Institute, Alexandria University, Alexandria, Egypt. [4]Cancer Management and Research Department, Medical Research Institute, Alexandria University, Alexandria, Egypt. [5]Immunology and Allergy Department, Medical Research Institute, Alexandria University, Alexandria, Egypt. *For Correspondence: shymaa.abdullah@alexu.edu.eg*

and involved in intercellular communication. Structurally, they are enclosed by a lipid bilayer membrane enriched with transmembrane tetraspanin proteins, as cluster of differentiation 63 (CD3), ALG-2-interacting protein-X (Alix), and tumor susceptibility gene-101 (TSG101). Moreover, the components of exosomes are a mixture of proteins, DNA, mRNAs, microRNAs, long noncoding RNAs, circular RNAs, and others. Functionally, as intercellular messengers, exosomes function to transfer diverse bioactive molecules from donor cells to recipient cells [7]. Exosomes are cell-derived membranous vesicles capable of transferring their cargo to recipient cells through membrane fusion. Consequently, exosomes and their molecular constituents play pivotal roles in modulating tumor growth, metastasis, and angiogenesis during cancer progression [8].

Therefore, the objective of the present study was to evaluate the proposed role of exosomes in the aggressiveness of TNBC cells. It assessed its role in influencing molecular mechanisms, such as autophagy, related to aggressive behavior via the *STAT3* signaling pathway in TNBC cells.

## Materials and Methods

*Cell lines*

Breast cancer cell lines MDA-MB-231 (mesenchymal-like; ATCC® HTB-26™), HCC1806 (basal-like; ATCC® CRL-2335™), and MCF-7 (estrogen receptor-positive; ATCC® CRL3435™) were sourced from ATCC (Manassas, Virginia, USA). The cells were grown in high-glucose Dulbecco's Modified Eagle Medium (DMEM), low-glucose DMEM, and RPMI1640 medium, respectively, enriched with 10% fetal bovine serum (FBS), 2mM glutamine, and 0.1mg/mL of penicillin and streptomycin, and kept at 37°C in an atmosphere of 5% CO2.

*Exosome separation*

A serum was collected from a TNBC patient (stage IV, grade III, metastatic) following confirmation of diagnosis and informed consent from the Medical Research Institute, Alexandria University Ethics Committee Ref. No. E/C.S/N.T94/2021. Exosomes were extracted utilizing a total serum exosome isolation kit (Invitrogen™ UAB), followed by purification through ultracentrifugation at 100,000xg for 90 minutes in 7.5 ml of phosphate-buffered saline (PBS), and subsequently resuspended in 400 µl of PBS.

*Cytotoxicity assay*

Cells were seeded at a density of 10,000 per well in 96-well plates and maintained at 37°C with 5% CO2 until they reached 80% confluence. They were then treated with various concentrations of AG490 and DOXO in 200 µl of complete media for 48 hours. After incubation, 10 µl of MTT solution (5 mg/mL) was introduced to the wells and incubated for an additional 4 hours at 37°C. The control wells consisted of 50 µl of cells combined with 50 µl of MTT solution. Afterward, the media was removed, and 100 µl of dimethyl sulfoxide (DMSO) was added to each well. The absorbance was recorded at 590 nm using an ELISA reader from BioTek Instruments, Inc., USA. Cell viability was evaluated using the trypan blue exclusion method at a ratio of 1:1. The half-maximal inhibitory concentration ($IC_{50}$) values were calculated from the relative viability data using Compusyn software (https://www.combosyn.com/). This experiment was conducted three times.

*Estimation of STAT3 signaling pathway inhibition*

Two subtypes of cell lines were treated with the $IC_{50}$ of AG490 for 48 hours. Total protein was extracted from 1x10^5 treated and untreated cells and measured using the BCA assay. Western blotting was then performed to assess *STAT3* signaling, using pan-*STAT3* antibody purchased from Wuhan Fine Biotech Co., Ltd., China, and phospho-*STAT3* antibody (Tyr705) from Cell Signaling Technology, USA. Computational analysis was conducted on blot membranes from all three cell lines, with at least two replicates analyzed per condition, both before and after inhibition.

*Experimental design*

Each cell line was classified into eight separate groups: (1) Untreated cells that received no treatment; (2) EXO-cells that treated with exosomes (20 µg protein equivalent, determined by exosome uptake assays); (3) DOXO-cells that exposed to the $IC_{50}$ dose of doxorubicin; (4) *EXO-DOXO*-cells that treated with 20 µg of EXO and the $IC_{50}$ dose of DOXO; (5) InST-cells that treated with the $IC_{50}$ dose of AG490, an inhibitor of the *STAT3* pathway; (6) InST-EXO-cells that InST-cells received 20µg of EXO; (7) InST-DOXO-cells that InST-cells treated with the $IC_{50}$ dose of DOXO; and (8) InST-*EXO-DOXO*-cells that InST-cells received both 20 µg of EXO and the $IC_{50}$ dose of DOXO. Cells were cultured at a density of 5x103 per well in 12-well plates with complete media at 37°C and 5% $CO_2$. The media was changed every 48 hours until the cells reached 80% confluence. Un-InST-cells were incubated with EXO and/or DOXO for 48 hours. InST-cells were pre-treated with AG490 for 48 hours, washed, and then incubated with EXO and/or DOXO at 37°C and 5% CO2 for 48 hours. Following incubation, cells were harvested with 0.2 ml trypsin-EDTA, centrifuged at 2000xg for 5 minutes, and then collected for downstream analysis.

*Cell cycle analysis*

Harvested cells (1 x $10^5$ cells) were suspended in 0.5 ml of PBS and then gradually added to 4.5 ml of cold 70% ethanol while gently vortexing. This mixture was maintained at 4°C for 2 hours, followed by centrifugation at 300 xg for 5 minutes. The cells were subsequently washed in PBS and subjected to further centrifugation at 300 xg for 5 minutes. A staining solution containing propidium iodide (PI) with 50 µl of RNase A (final concentration of 0.5 µg/ml) was added to the cell pellets, mixed thoroughly, and incubated for a minimum of 4 hours at 4°C. The cells were then analyzed utilizing flow cytometry with 488 nm laser illumination.

*Analysis of apoptosis*

Cells were harvested at a density of 1x10^5 and rinsed twice with 1 ml of 1x Annexin-binding buffer. They were then centrifuged at 300 xg for 5 minutes and resuspended in the same buffer. Next, Annexin-V reagent was added, mixed thoroughly, and incubated in the dark at room temperature for 15 minutes. The PI solution was added, mixed, and incubated in the dark at room temperature for 5 minutes. After incubation, 400 µl of 1× Annexin-binding buffer was added, and the sample was analyzed using flow cytometry. Untreated cells were used as a negative control to determine the basal level of apoptotic, necrotic, and dead cells.

*Monitoring of autophagic machinery stages*

The overall autophagic machinery in the utilized cell lines was assessed by microtubule-associated protein 1 light chain 3 beta (LC3B) protein level according to the manufacturer's instructions (Wuhan Fine Biotech Co., Ltd.) using the ELISA technique.

Furthermore, a relative quantitative reverse transcription polymerase chain reaction (qRT-PCR) was performed to measure the expression levels of specific autophagy-related genes, such as *BECLIN1, ATG16L1, ATG5*, and *RAB24.* Table 1 Total RNA was extracted from the collected cells using the GENEzol™ TriRNA Pure Kit (Geneaid Biotech Ltd., Taiwan) and then reverse-transcribed into complementary DNA (cDNA) with the HiSenScript™ RH(–) cDNA Synthesis Kit (iNtRON Biotechnology, Korea). Each PCR mixture included 10 µl of TOPreal™ Master Mix, 2 µl of cDNA, and 0.5 µM of each primer, resulting in a final volume of 20 µl. Amplification was conducted under the following thermal parameters: an initial denaturation step at 95 °C for 10 minutes, followed by 45 cycles consisting of 95 °C for 15 seconds, 56 °C for 15 seconds, and 72 °C for 30 seconds. qRT-PCR assessments were executed using an Applied Biosystems™ 7500 Real-Time PCR System (Thermo Fisher Scientific, USA). Relative mRNA expression was determined utilizing the comparative threshold cycle ($2^{-\Delta\Delta CT}$) method, with *GAPDH* acting as the internal reference gene.

*Statistical analysis*

Statistical evaluations were performed utilizing SPSS software version 22.0 (IBM Corp., Armonk, NY, USA). To compare the average values of various biochemical parameters across groups, the Mann–Whitney U test, which is a nonparametric method, was employed. A p-value of ≤ 0.05 was deemed statistically significant.

## Results

*Cytotoxicity test*

Treatment with AG490 and DOXO for 48 hours reduced the growth of TNBC and NTNBC cells compared to the untreated controls, displaying significantly different effects as described in Table 2 [9]. The results indicated that MDA-MB-231 cells were more sensitive to both AG490 and DOXO compared to the other two cell lines.

*Estimation of STAT3 signaling pathway inhibition*

Western blot analysis showed reduced p-*STAT3* expression relative to pan-*STAT3* following AG490 treatment. Quantitative assessment of inhibition demonstrated that MCF-7 cells exhibited the highest level of suppression (91.5%), compared with 74% in HCC1806 and 66.4% in MDA-MB-231 cells [9].

*Cell morphology*

Exosome treatment caused TNBC cells to adopt an elongated, spindle-like shape, whereas NTNBC cells formed aggregates and clumps in comparison to the untreated controls. The application of DOXO led to the formation of rounded, detached cells and cellular debris in both MDA-MB-231 and MCF-7 cell lines, with MCF-7 cells showing a more pronounced effect. On the other hand, HCC1806 cells did not display any noticeable morphological changes. Importantly, when compared to DOXO alone, TNBC cells treated with *EXO-DOXO* presented more elongated, spindle-like morphologies. Additionally, NTNBC cells exhibited cellular aggregates and clumps Figure 1.

Exosome treatment reduced the spindle-shaped cells in the inhibited MDA-MB-231 cells, but it decreased the presence of small circular vacuoles in InST-HCC1806 cells. In the inhibited MCF-7 cells, the treatment led to the loss of cellular aggregates and clumps compared to the cells treated with exosomes. The DOXO treatment on InST-TNBC and InST-NTNBC cells did not show

Table 1. The Sequence of Primers of Targeted Genes in the Autophagic Machinery

| Gene | Primer sequence (5′-3′) | Accession number |
|---|---|---|
| *BECLIN-1* | Forward: 5′-ACCGTGTCACCATCCAGGAA-3′ | NM_003766.5 |
| | Reverse :5′-GAAGCTGTTGGCACTTTCTGT-3’ | |
| *ATG16L1* | Forward:: 5, AGGGTTCCCTATCTGGCAGT-3′ | NM_001363742.2 |
| | Reverse : 5′-GATTCGGCTTGCAAAATCAT-3′ | |
| *ATG5* | F: 5′-TGGCCATCAATCGGAAACTC-3′ | NM_004849.4 |
| | R: 5′- CAGCCACAGGACGAAACAG-3′ | |
| *RAB24* | Forward: 5’-CCGAGCGGAGATCGGGGTTTGC-3′ | |
| | Reverse: 5-AGAGGACCTGGGGTAGCTCAGA-3′ | NM_001031677.3 |
| *β-actin* | F: 5’-TGGCACCACACCTTCTACAATGAGC-3’ | NM_001101.5 |
| | R: 5’-GCACAGCTTCTCCTTAATGTCACGC-3’ | |

*ATG16L1*, Autophagy Related 16 Like 1; *ATG5*, Autophagy related gene 5; *RAB24*, Ras-related protein

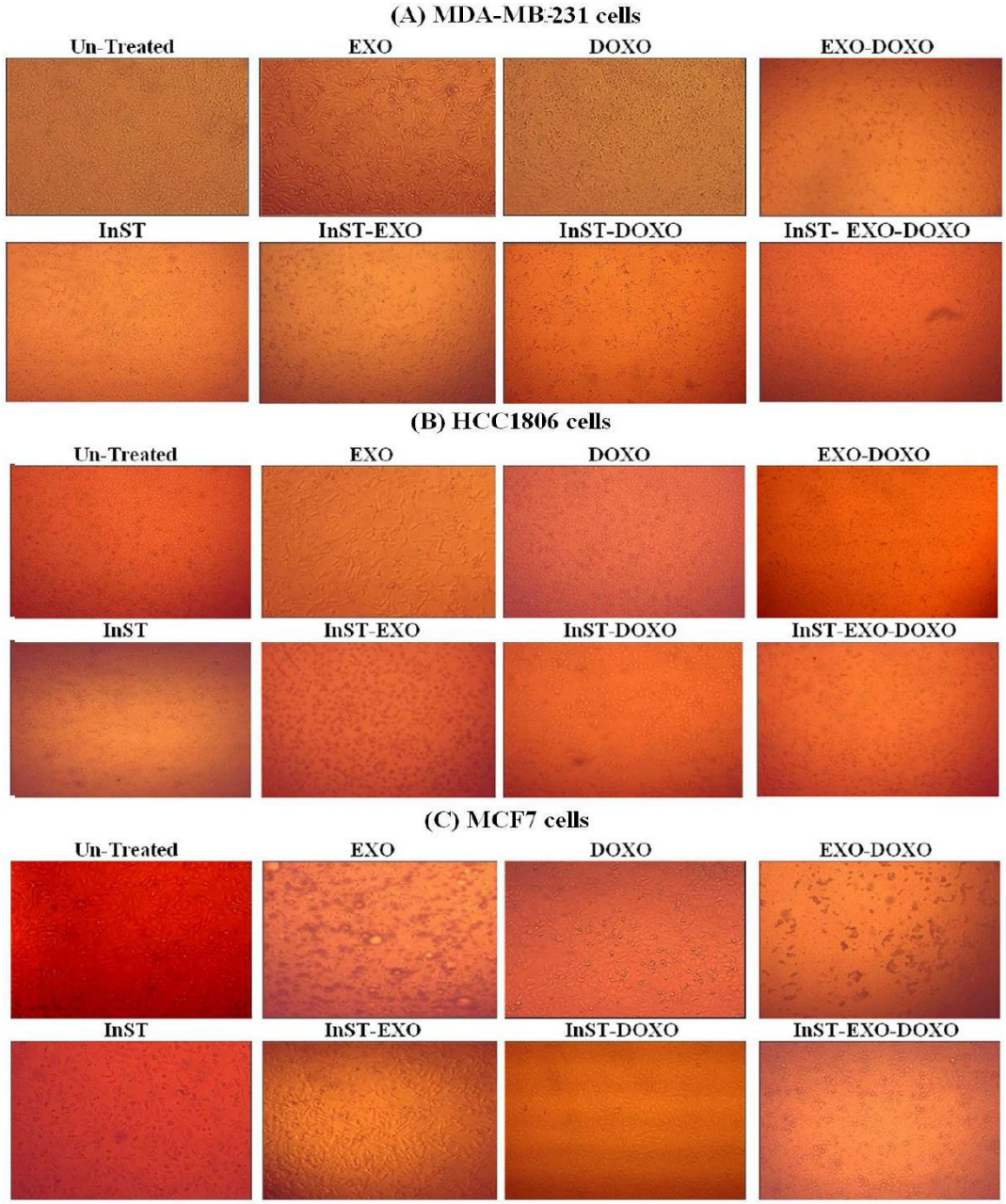


Figure 1. Morphological Alterations in the Utilized Cell Lines after Exosomes and/or Doxorubicin Treatment for 48 hrs Related to *STAT3* Pathway Inhibition

any noticeable changes under the microscope, but it did decrease cell viability compared to the untreated samples. *EXO-DOXO* did not cause any morphological changes in InST-MDA-MB-231 cells in relation to the *EXO-DOXO*-treated cells. Conversely, it presented an elongated spindle shape when compared to the InST-DOXO-treated cells. Additionally, in InST-HCC1806 cells, the introduction of *EXO-DOXO* still led to a reduction in the size of small circular vacuoles compared to those found in *EXO-DOXO*- and InST-DOXO-treated cells. In InST-MCF-7 cells, the clusters and aggregates present in *EXO-DOXO*-treated cells were absent. Additionally, when compared to InST-DOXO-treated cells, InST-MCF-7 cells that received *EXO-DOXO* exhibited small circular vacuoles. Figure 1.

Table 2. The Half Maximal Inhibitory Concentration ($IC_{50}$) Values of AG490 and DOXO treatments against. a, MDA-MB-231; b, HCC1806, and MCF-7 cells after 48 hours

| Cell lines | $IC_{50}$ value of AG490 | $IC_{50}$ value of DOXO |
|---|---|---|
| MDA-MB-231 cells | 25.4±0.009 µM | 1.72±0.001 µM |
| HCC1806 cells | 44.16±0.026 µM | 15. 17±0.003 µM |
| MCF-7 cells | 96.07±0.042 µM | 8.34±0.009 µM |

$IC_{50}$, Half maximal inhibitory concentration; DOXO, Doxorubicin

*Cell cycle analysis*

The impact of exosomes and/or doxorubicin treatment on the distribution of the cell cycle within the selected cell lines, prior to and following *STAT3* pathway inhibition, is illustrated in Figure 2.

Table 3. Statistical Analysis of LC3B Levels (ng/ml) in the Utilized Cell Lines after Different Treatments were Administered for 48 hrs

| Cell lines | MDA-MB231 | HCC1806 | MCF-7 |
|---|---|---|---|
| Groups | Mean ± S.E. | Mean ± S.E. | Mean ± S.E. |
| | UN-InST cells | | |
| Un-Treated | 0.46 ± 0.02 | 0.20 ± 0.011 | 0.25 ± 0.006 |
| EXO | 0.63 ±0.044 [a] | 0.25 ± 0.002 [a] | 0.36 ± 0.003 [a] |
| DOXO | 0.59 ± 0.002 [a] | 0.18± 0.006 | 0.41 ± 0.003 [a] |
| EXO-DOXO | 0.98 ±0.078 [c] | 0.21 ± 0.013 | 0.43 ± 0.008 |
| | InST cells | | |
| InST | 0.44 ± 0.011 | 0.17 ± 0.006 | 0.49 ± 0.032 |
| InST-EXO | 0.63 ± 0.029 | 0.20 ± 0.033 [b] | 0.41 ± 0.005 [b] |
| InST-DOXO | 0.44 ± 0.006 [c] | 0.18 ± 0.013 | 0.51 ± 0.004 [c] |
| InST- EXO-DOXO | 0.47 ± 0.014 [d] | 0.17 ± 0.006 [d] | 0.56 ± 0.018 [d,e] |

EXO, Exosomes; DOXO, Doxorubicin; InST, inhibited STAT3 cells; S.E, Standard Erro; [a], statistically significant difference compared to the untreated control group; [b], statistically significant difference compared to the EXO-treated group; [c], statistically significant difference compared to the DOXO-treated group; [d], statistically significant difference compared to the EXO-DOXO-treated group; [e], statistically significant difference compared to the InST-DOXO-treated group; p-values ≤ 0.05 were considered to indicate statistical significance

*Analysis of apoptosis*

The consequence of exosomes and/or doxorubicin treatment on the percentages of early and late apoptotic and necrotic cells in the cell lines used, both prior to and following the inhibition of the *STAT3* pathway, is shown in Figure 3.

*Monitoring stages of the autophagic machinery*

The biochemical results indicated that the LC3B level was highest in MDA-MB-231 cells, followed by MCF-7 and HCC1806 cells. Treatment with EXO significantly increased the LC3B level in both TNBC and NTNBC cells ($p < 0.05$) compared to untreated cells. However, DOXO treatment significantly increased the LC3B level in MDA-MB-231 and MCF-7 cells ($p < 0.05$), but no significant changes were seen in HCC1806 cells ($p > 0.05$). Notably, when comparing DOXO treatment to *EXO-DOXO* treatment, the latter resulted in a notable increase in LC3B level only in MDA-MB-231 cells ($p < 0.05$) Table 3.

In comparison to EXO-treated cells, exosome treatment did not alter the LC3B level in InST-MDA-MB-231 cells, whereas it was significantly reduced in InST-HCC1806 cells ($p \leq 0.05$); conversely, its level in InST-MCF-7 cells significantly increased ($p \leq 0.05$). When compared to DOXO-treated cells, DOXO treatment led

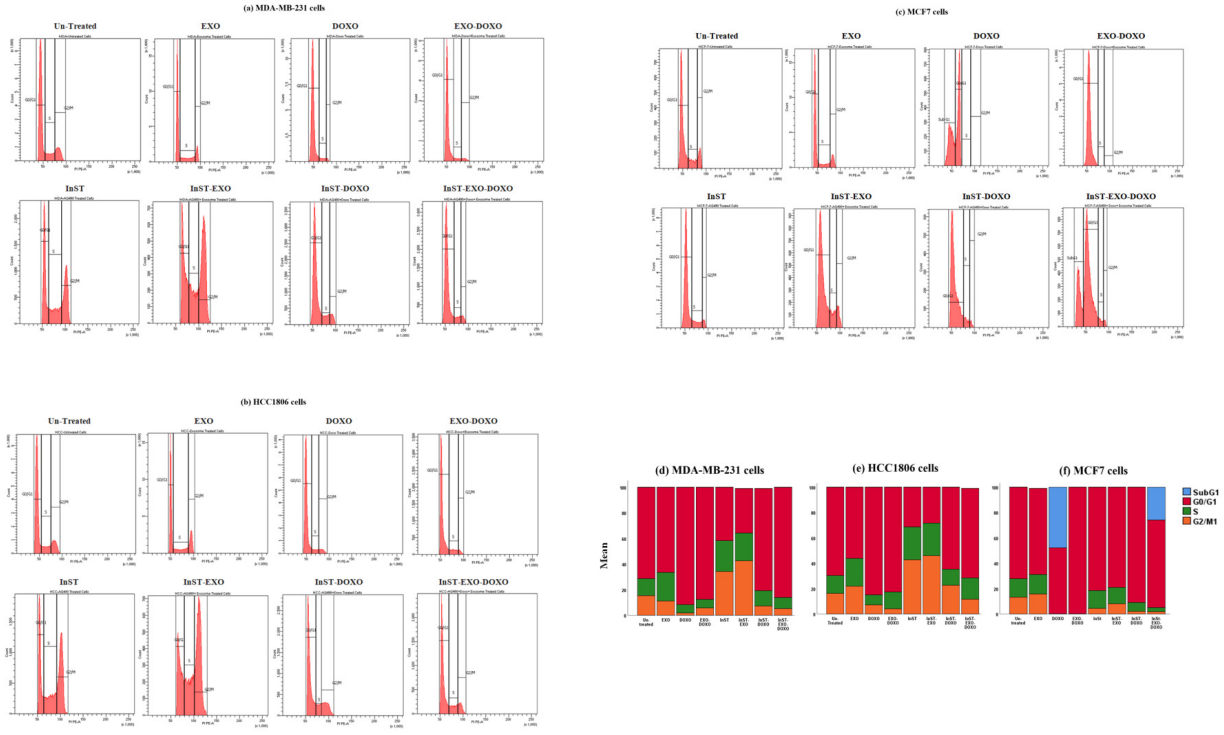


Figure 2. Cell Cycle Analysis of the Utilized Cell Lines after Exosomes and/or Doxorubicin Treatment for 48 hrs Related to *STAT3* Pathway Inhibition

Table 4.Statistical Analysis of Targeted Gene Expression (Fold Change) of the Autophagic Machinery in the Utilized Cell lines after EXO or/and DOXO Administration for 48 hr before and after *STAT3* Pathway Inhibition

| Groups | *BECLIN1* | *ATG16L* | *ATG5* | *RAB24* |
|---|---|---|---|---|
| | MDA-MB231 cells | | | |
| | Mean ±S.D. | Mean ±S.D. | Mean ±S.D. | Mean ±S.D. |
| Un-Treated | 1.00 ± 0.09 | 1.02 ± 0.15 | 1.00 ± 0.06 | 1.01 ± 0.10 |
| EXO | 0.97 ± 0.17 | 0.27 ± 0.01[a] | 1.49 ± 0.16[a] | 1.48 ± 0.05[a] |
| DOXO | 1.07 ± 0.04 | 0.92 ± 0.20 | 1.82 ± 0.11[a] | 0.90 ± 0.17 |
| DOXO-EXO | 0.90 ± 0.04 | 0.21 ± 0.02[b] | 1.90 ± 0.05 | 1.44 ± 0.27 |
| InST-EXO | 0.17 ± 0.01[c] | 0.42 ± 0.03[c] | 0.44 ± 0.07[c] | 1.79 ± 0.15 |
| InST-DOXO | 0.66 ± 0.15[b] | 2.0 ± 0.33[b] | 1.59 ± 0.27 | 2.45 ± 0.15[b] |
| InST-EXO-DOXO | 0.23 ± 0.02[d,e] | 1.74 ± 0.07[d] | 0.55 ± 0.06[d,e] | 2.21 ± 0.20 |
| | HCC1806 cells | | | |
| | Mean ±S.D. | Mean ±S.D. | Mean ±S.D. | Mean ±S.D. |
| Un-Treated | 1.00 ± 0.06 | 1.00 ± 0.03 | 1.00 ± 0.04 | 1.00 ± 0.10 |
| EXO | 0.40 ± 0.03[a] | 0.14 ± 0.01[a] | 0.92 ± 0.15 | 0.17 ± 0.01[a] |
| DOXO | 0.65 ± 0.08[a] | 0.97 ±0.05 | 1.21 ± 0.09 | 0.25 ± 0.01[a] |
| EXO-DOXO | 0.38 ± 0.04[b] | 1.18 ± 0.05 | 1.88 ± 0.31 | 0.32 ± 0.01 |
| InST-EXO | 0.22 ± 0.05[c] | 0.49 ± 0.08[c] | 0.59 ± 0.01[c] | 0.12 ± 0.01 |
| InST-DOXO | 0.51 ± 0.05 | 1.26 ± 0.09 | 1.07 ± 0.04 | 0.22 ± 0.02 |
| InST-EXO-DOXO | 0.28 ± 0.04[e] | 1.06 ± 0.05 | 0.85 ± 0.08[d,e] | 0.13 ± 0.01[d,e] |
| | MCF-7 cells | | | |
| | Mean ±S.D. | Mean ±S.D. | Mean ±S.D. | Mean ±S.D. |
| Un-Treated | 1.00 ± 0.03 | 1.00 ± 0.02 | 1.01 ± 0.09 | 1.01 ± 0.12 |
| EXO | 1.26 ± 0.13 | 0.59 ± 0.04[a] | 0.63 ± 0.04 | 0.93 ± 0.05 |
| DOXO | 2.67 ± 0.12[a] | 0.94 ± 0.20 | 1.08 ± 0.09 | 1.42 ± 0.31 |
| EXO-DOXO | 1.64 ± 0.03[b] | 1.04 ± 0.03 | 1.16 ± 0.12 | 1.41 ± 0.10 |
| InST-EXO | 2.7 ± 0.63[c] | 2.08 ± 0.14[c] | 1.01 ± 0.07[c] | 4.38 ± 1.19[c] |
| InST-DOXO | 3.89 ± 0.38[b] | 1.89 ± 0.36[b] | 1.95 ± 0.29[b] | 2.11 ± 0.03[b] |
| InST-EXO-DOXO | 3.93 ± 0.52[d] | 1.88 ± 0.04[d] | 1.97 ± 0.22[d] | 3.20 ± 0.95[d] |

EXO, Exosomes; DOXO, Doxorubicin; InST, inhibited *STAT3* cells; S.E, Standard Error; [a], statistically significant difference compared to the untreated control group; [b], statistically significant difference compared to the EXO-treated group; [c], statistically significant difference compared to the DOXO-treated group; [d], statistically significant difference compared to the EXO-DOXO-treated group; [e] ,statistically significant difference compared to the InST-DOXO-treated group. p-values ≤ 0.05 were considered to indicate statistical significance

to a significant decrease in LC3B level in InST-MDA-MB-231 cells (p≤0.05), had no substantial effect on InST-HCC1806 cells (p > 0.05), and caused a significant increase in its level in InST-MCF-7 cells (p≤0.05).

Exosomes with doxorubicin treatment significantly decreased LC3B level in InST-MDA-MB-231 and InST-HCC1806 (p≤0.05) but significantly increased its level in InST-MCF-7 cells (p≤0.05) compared to cells treated with Exosomes and doxorubicin without inhibition. On the other hand, compared to InST-DOXO-treated cells, it did not significantly alter its levels in InST-TNBC (p>0.05) but significantly increased its level in InST-MCF-7 cells (p≤0.05) (Table 3).

In the molecular analysis, treating MDA-MB-231 cells with EXO led to a significant downregulation of ATG16L and an upregulation of *ATG5* and *RAB24* expression (p ≤ 0.05) compared to untreated cells. Furthermore, in HCC1806 cells, EXO treatment significantly downregulated the expression of *BECLIN1*, ATG16L, and *RAB24* (p ≤ 0.05). In MCF-7 cells, exosome treatment resulted in a significant decrease in the expression of ATG16L only (p ≤ 0.05) (Table 4).

On the other hand, compared to untreated cells, DOXO treatment in MDA-MB-231 cells exhibited significant upregulation of *ATG5* expression (p≤0.05). However, HCC1806 cells exhibited significant downregulation of *BECLIN1* and *RAB24* expression (p≤0.05). Interestingly, in the MCF-7 cells, it significantly upregulated *BECLIN1* expression only (p≤0.05) (Table 4).

Moreover, in TNBC cells, *EXO-DOXO*-treated cells presented a significant reduction in ATG16L and *BECLIN1* expression (p≤0.05); moreover, treatment of NTNBC cells significantly reduced *BECLIN1* expression (p≤0.05) compared to cells treated with DOXO treatment alone (Table 4).

The inhibitory effect of ATG490 differed between TNBC and NTNBC cells. In InST-TNBC cells, EXO treatment significantly decreased *BECLIN1* and *ATG5* expression (p≤0.05) and increased ATG16L expression. Interestingly, in NTNBC cells, it significantly increased

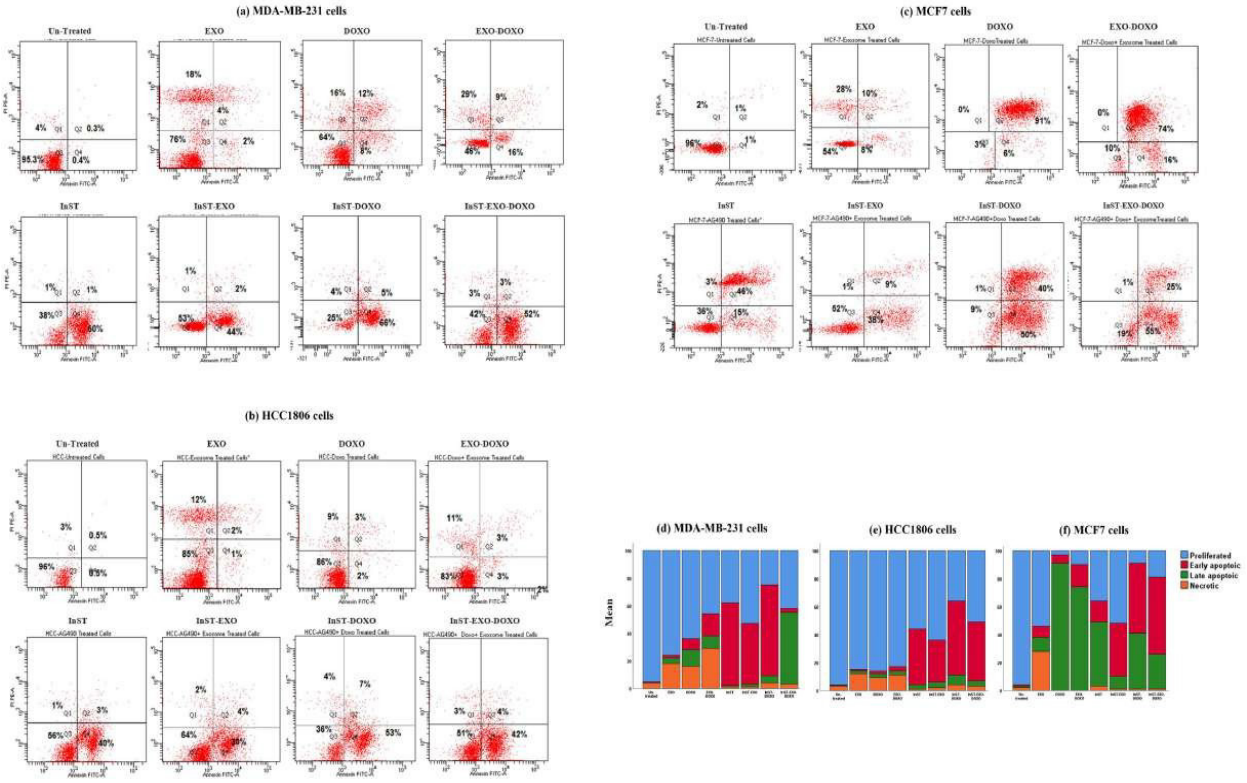


Figure 3. Analysis of Apoptotic Cells after Exosomes and/or Doxorubicin Treatment for 48 hrs Related to *STAT3* Pathway Inhibition

the expression of all genes ($p \leq 0.05$) compared to un-InST cells (Table 4).

DOXO treatment of InST-MDA-MB-231 cells, compared to cells treated with DOXO, significantly downregulated *BECLIN1* and upregulated ATG16L and *RAB24* expression ($p \leq 0.05$). In InST-HCC1806 cells, there was no significant change in all gene expression. On the other hand, in InsT-MCF-7 cells, all gene expressions were remarkably upregulated ($p \leq 0.05$) (Table 4).

In InST-MDA-MB-231 cells, the expression levels of *BECLIN1* and *ATG5* were significantly lower compared to the *EXO-DOXO* cells without *STAT3* inhibition, while ATG16L expression was higher ($p \leq 0.05$). Conversely, when comparing InST-DOXO cells, the expression of both ATG16L and *ATG5* was significantly lower ($p \leq 0.05$). In InST-HCC1806 cells, *ATG5* and *RAB24* expression was lower than in *EXO-DOXO*-treated cells without inhibition. In comparison to the InST-DOXO cells, the expressions of *BECLIN1*, *ATG5*, and *RAB24* were lower in the other cell line. In the InsT-MCF-7 cells, treatment with *EXO-DOXO* significantly increased the expression of all genes when compared to cells treated with *EXO-DOXO* without *STAT3* inhibition. However, there were no significant differences in gene expressions between the *EXO-DOXO*-treated cells and the InST-DOXO-treated cells (Table 4).

## Discussion

Exosome uptake assays revealed that the metabolic state of recipient cells affects their ability to internalize exosomes, with metabolically active cells such as stem cells showing greater rates of uptake compared to fully differentiated cells [10]. The substantial exosome uptake noted in MDA-MB-231 cells may be linked to their mesenchymal-like phenotype and invasive traits characteristic of TNBC, which aligns with their higher expression of markers related to epithelial–mesenchymal transition (EMT) and stem cells. HCC1806 cells exhibited relatively lower uptake, indicative of their more differentiated status and luminal or basal-like morphological characteristics. MCF-7 cells, identified as part of the luminal-A subtype, showed the least exosome uptake, reflecting their advanced level of differentiation and reduced migratory ability due to strong cell–cell junctions [10]. Besides, TNBC has been reported to acidify its extracellular microenvironment, thereby facilitating its aggressive phenotype [11]. One way that exosomes are taken up by recipient cells is through membrane fusion with the plasma membrane, a process that requires an acidic pH [12]. Furthermore, the present study demonstrated that TNBC-derived exosomes are preferentially internalized by TNBC cells compared to non-TNBC cells and concluded that the uptake of exosomes may depend on their origin and receipt [9, 13].

Morphologically, treating TNBC cells with exosomes aligns with earlier research, which indicates that the introduction of exosomes derived from TNBC can lead to alterations in the shape of recipient TNBC cells, resulting in more polarized forms and an increase in cell area, reflective of motile characteristics [9, 14]. Moreover, the findings from treating NTNBC with exosomes correspond with a prior study that indicated that TNBC-derived exosomes could influence MCF-7 cells by triggering a reduction in cell stiffness, rearranging the cytoskeleton

and focal adhesions, as well as modifying cellular morphology [9, 15] Remarkably, previous evidence has demonstrated the capability of exosomes to establish intercellular connections and form multicellular clusters within recipient cells [9, 16].

The morphological alterations caused by DOXO were more significant in NTNBC cells than in TNBC cells, with a higher degree of apoptosis observed in MCF-7 cells compared to MDA-MB-231 cells. Conversely, cytotoxicity tests indicated that MDA-MB-231 exhibited greater sensitivity to DOXO than MCF-7, aligning with findings from prior studies. DOXO triggers apoptosis by activating death signaling pathways in susceptible breast cancer cell lines [17]. An assessment of MDA-MB-231 cells revealed cells that were rounded, condensed, and detached, while HCC1806 cells showed minimal signs of cell death. These results are in agreement with earlier studies that suggest the mesenchymal subtype of TNBC is more responsive to DOXO than other TNBC subtypes, such as the basaloid variant [9, 18,19].

In comparison to DOXO treatment by itself, TNBC cells treated with *EXO-DOXO* exhibited elongated and spindle-like shapes. Likewise, NTNBC cells with *EXO-DOXO* postponed the development of cell aggregates and clusters. Together, these results offer additional proof of the involvement of exosomes in facilitating the chemoresistance of breast cancer cells to DOXO [19].

AG490 inhibited the *STAT3* pathway in breast cancer cell lines, showing the strongest effect in MCF-7 cells and the weakest in MDA-MB-231 cells. The level of *STAT3* inhibition was inversely related to the sensitivity of cell lines to AG490. Exosome treatment had different effects; it reduced spindle-shaped cells in InST-MDA-MB-231 cells and eliminated cell aggregates in InST-MCF-7 cells. InST-HCC1806 cells treated with exosomes exhibited a combination of small circular cells, along with increases in both cell viability and cell death. Overall, AG490 enhanced antitumor effects through *STAT3* inhibition, with the tumorigenic effects of exosomes possibly linked to *STAT3* signaling [9]. Adding DOXO to AG490-treated TNBC and NTNBC cells increased the cytotoxicity of DOXO, resulting in greater cell death. This finding, along with the previously demonstrated chemotherapeutic potential of AG490, suggests that inhibiting *STAT3* in combination with DOXO treatment may enhance the effectiveness of antitumor strategies in breast cancer cells [9, 20].

The treatment of InST-MDA-MB-231 cells with exosomes and Doxo did not exhibit additional morphological changes; however, elongated spindle-shaped cells were observed compared to the InST-DOXO treatment. In InST-HCC1806 cells, *EXO-DOXO* led to a greater persistence of small, circular cells. Conversely, in InST-MCF-7 cells, *EXO-DOXO* treatment resulted in the disappearance of cellular aggregates compared to *EXO-DOXO* alone. Notably, InST-MCF-7 cells treated with *EXO-DOXO* maintained their small, circular morphology, supporting earlier findings that AG490 decreases phosphorylated *STAT3* levels, reducing cancer cell adhesion and invasion [21, 22]. The observations suggest that exosomes play a role in enhancing tumorigenic behaviors and chemoresistance in breast cancer, particularly in TNBC.

Analysis of the cell cycle in TNBC cells treated with exosomes revealed an increase in the cell population arrested at the S phase compared to that in untreated cells. During that phase, DNA replication occurs, which is considered an irreversible commitment to cell proliferation [23]. Moreover, an apoptotic assay revealed rise in necrotic cells, which is associated with tumor progression and aggressiveness [24]. Consequently, swelling of necrotic cells and the subsequent release of cytoplasmic contents into the extracellular space may trigger inflammatory responses, thereby increasing the likelihood of proto-oncogenic mutations or epigenetic alterations that promote angiogenesis, cancer cell proliferation, invasion, epithelial–mesenchymal transition (EMT), and metastasis [25]. Consistent with the findings of the current study, the capacity of exosomes derived from breast cancer cells to enhance tumor progression by increasing cell proliferation and inhibiting apoptosis in recipient cells has been documented [26]. Thus, the results of this research confirm the role of exosomes in enhancing the tumorigenic behavior of NTNBC and TNBC cells.

Cell cycle analysis of TNBC cells treated with DOXO revealed a cell population arrested at the Go/G1, indicating its proapoptotic effect [27]. Additionally, apoptosis assays revealed an increase in late apoptotic and necrotic MDA-MB-231 cells, while HCC1806 cells demonstrated necrosis. Previously, the ability of DOXO to promote the production of high levels of reactive oxygen species (ROS), which cause damage to cellular membranes, DNA, and proteins, has been demonstrated. This, in turn, is closely associated with necrotic and apoptotic cell death signaling pathways [28]. However, treatment of NTNBC cells with DOXO led to an increase in the number of cells arrested at the subG1, revealing its proapoptotic effect [29]. The wild-type p53 gene is activated in MCF-7 cells following DOXO treatment, leading to cell cycle arrest in the subG1 phase [30]. In contrast, this gene is mutated and nonfunctional in MDA-MB-231 cells [31].

In comparison to cells treated with DOXO, the analysis of apoptosis in TNBC cells treated with *EXO-DOXO* showed an increase in necrotic cells. Additionally, cell cycle analysis of MDA-MB-231 cells revealed a rise in cell cycle arrest at the G2/M phase, indicating progression through the cell cycle. It is important to note that the decision to complete cell division can occur during the G2 phase in actively proliferating cells [21, 32]. Furthermore, the arrest of HCC1806 cells in the S phase indicated cell cycle progression, suggesting that the cells were proliferating. In MCF-7 cells treated with *EXO-DOXO*, there was an increase in the proportion of cells arrested in the G0/G1 phase, along with a decrease in the percentage of apoptotic cells and an increase in proliferative cells. These results may support the role of exosomes in enhancing the tumorigenic behavior of recipient breast cancer cells, particularly in promoting chemoresistance to DOXO treatment [10].

However, after treating InST-TNBC and InST-NTNBC cells with exosomes, the apoptosis assay revealed an increase in apoptotic cells, accompanied by a decrease in

proliferative cells compared to that in the EXO-treated cells. Notably, these findings are compatible with those of the proliferative assay. Moreover, in contrast to that in InST-NTNBC cells, cell cycle analysis of InST-TNBC cells revealed an increase in the proportion of cells arrested at the G2/M phase associated with a decrease in the G0/G1 phase compared to that in Un-InST cells. These findings suggest that the uptake and tumorigenic role of exosomes are more pronounced in TNBC cells compared to NTNBCs, potentially due to the source of exosomes or the type of recipient cells [8, 9, 13].

In comparison to cells treated with DOXO alone, InST-TNBC and InST-NTNBC cells that received DOXO were more prone to undergoing apoptosis. Garibaldi et al. previously demonstrated that blocking the *STAT3* signaling pathway enhances the sensitivity of breast cancer cells to the pro-apoptotic effects of DOXO, albeit to varying degrees [33]. Nonetheless, in InST-TNBC cells, an increase in the population of cells arrested in both the G2/M and S-phases should also be taken into account, as this may indicate the chemoresistance characteristic of TNBC cells [34]. When InST-TNBC cells were treated with DOXO, the number of proliferative cells decreased compared to treatment with DOXO alone.

In addition, an assay for apoptosis conducted on InST-TNBC and InST-NTNBC cells that were treated with *EXO-DOXO* indicated that the majority of cells were in the apoptotic phase when compared to *EXO-DOXO*-treated cells without any inhibition. These findings may suggest that AG490 has an anticancer effect by promoting apoptosis in breast cancer cells [35, 36]. Therefore, even though AG490 was utilized as a *STAT3* inhibitor, its anticancer properties should not be overlooked. Furthermore, the distribution of the cell cycle in InST-MDA-MB-231 cells treated with *EXO-DOXO* showed an increase in the number of cells that were halted in the S phase. In addition, in InST-HCC1806 cells exposed to *EXO-DOXO*, there was a noted rise in cells that were stalled in both the G2/M and S phases. These results might be linked to the high growth rate and drug resistance exhibited by TNBC cells [34, 37]. Conversely, when considering the extent of *STAT3* inhibition in NTNBC and TNBC cells, it was found that *STAT3* inhibition was more pronounced in NTNBC cells than in TNBC cells, while the cell cycle distribution of InST-MCF-7 cells treated with *EXO-DOXO* revealed an increase in cells that were arrested at sub-G1.

However, compared with InST-DOXO-treated cells, proliferative cells were increased in InST-TNBC and InST-NTNBC cells treated with *EXO-DOXO* treatment. This observation may contribute to the role of exosomes in potentiating the tumorigenic behavior of breast cancer. On the other hand, cell cycle analysis of InST-TNBC cells treated with *EXO-DOXO* revealed an increase in G0/G1 cell arrest compared to that in InST-DOXO-treated cells. Moreover, in the case of InST-NTNBC cells, an increase in the number of cells arrested in the subG1 phase was observed compared to that in InST-DOXO-treated cells. Previously, combination therapy with AG490 and DOXO may have induced greater antitumor effects in breast cancer cells than single agents alone [33, 38].

On the other hand, autophagy is an internal defensive mechanism that allows cells to survive under different stressors and has dual roles in tumor promotion and suppression [3]. The results of exosome treatment of TNBC or NTNBC cells showed a statistically significant effect on the autophagic machinery compared to untreated cells. Previously, it was reported that exosomes derived from breast cancer may play an essential role in promoting autophagy via ROS production, which promotes tumorigenesis in recipient cells [39]. Additionally, it has been reported exosomes may exert cytoprotection by inducing intracellular autophagy [40]. Although autophagy may enhance tumorigenic behavior in breast cancer cells, other crucial factors may influence the Essential role of autophagy, e.g., The tumor type, stage of tumorigenesis, and the nature and magnitude of the insult to tumor cells [41].

This study showed that treating breast cancer cells with exosomes significantly increased the level of LC3B, which may indicate an enhancement of the autophagic machinery or an accumulation of LC3B in those cells. However, the observed molecular changes in MDA-MB-231 cells due to exosome treatment may represent an ideal example of enhanced autophagy, as exosomal uptake was most pronounced in these cells. This supposition may be supported by the significant upregulation of *ATG5* expression, which is indispensable for autophagic vesicle formation; previously, it was reported that *ATG5* knockdown results in the downregulation or total inhibition of autophagy [42]. Additionally, *RAB24* is an atypical RAB protein required for the clearance of late autophagic vacuoles under basal conditions and has also been connected to different pathological conditions, including tumor induction [43]. Moreover, ATG16L overexpression may cause an indirect effect on autophagy, and its overexpression inhibits autophagosome formation [3]. In line with these findings, the present study showed a decrease in ATG16L expression, which may partly explain the significant increase in LC3B levels in these cells and the heightened autophagy. Notably, the highest level of LC3B was observed in MDA-MB-231 cells.

After treating HCC1806 cells with exosomes, in addition to the significant rise in LC3B level, significant decreases in *BECLIN1*, ATG16L, and *RAB24* expressions were observed compared to those in untreated cells. These results are consistent with those of a previous study in which the LC3B level was significantly increased after *BECLIN1* was inhibite. *BECLIN1* downregulation due to exosome treatment should not delay the role of exosomes in enhancing autophagic tumorigenesis, since it has been shown that *BECLIN1* expression coincidentally regulates the autophagy process. It is assumed that there could be an undiscovered important protein regulating the autophagy process, and a possible negative feedback or two-way regulatory mechanism may play a role when *BECLIN1* expression is inhibited [44]. Additionally, *RAB24* expression was significantly downregulated, likely due to a slowdown or inhibition of autophagic flux. Previous research has indicated that autophagy can be inhibited at any stage of the autophagic process [45]. When the later stages of autophagy are

blocked, autophagosomes can build up in large quantities. Consequently, an increased number of autophagosomes after treatment with a particular stimulus may indicate either heightened autophagic activity (meaning more autophagosome formation) or a disruption in the process of autophagy at the lysosomal fusion stage [46]. In other words, the rise in LC3B levels following any treatment, such as exosomes in this study, may suggest either increased autophagosome formation, leading to enhanced autophagic degradation, or decreased autophagic turnover, resulting in autophagosome accumulation [47].

DOXO treatment of MDA-MB-231 cells may reflect the increase in autophagic machinery. Several studies have shown the cytoprotective role of autophagy in MDA-MB-231 cells in response to DOXO treatment [48, 49]. In HCC1806 cells, results align with Vu et al.'s recent report indicating that the protein expression level of *BECLIN1* decreased after treatment with DOXO at concentrations above 0.5 μM [50]. This result was consistent with the cytotoxicity test of DOXO in HCC1806 cells. However, the role of autophagy in HCC1806 cells in response to DOXO treatment is unclear and may suggest other causes of cell death. Regarding MCF-7 cells, the observed results potentially indicate an upregulation of autophagy, which may partially account for the previously reported increase in DOXO-induced cell death [50]. However, overall, the findings of the present work may provide additional evidence for the dual paradoxical role of autophagy in combination with therapeutic anticancer drugs, which can either induce cell death or promote cell survival [48].

The outcomes following treatment with *EXO-DOXO* in MDA-MB-231 cells, as opposed to those treated with DOXO, may indicate an enhancement in autophagy. Furthermore, while the effects of DOXO treatment are significant, these molecular alterations might be primarily influenced by the treatment with exosomes. Interestingly, the results observed in HCC1806 and MCF-7 cells may be associated with autophagic degradation [51]. Additionally, these observations could be corroborated by in vivo studies that demonstrated a reduction in autophagic vacuole formation due to *BECLIN1* deficiency [52]. Therefore, these findings imply that *EXO-DOXO* treatment might inhibit autophagic flux in HCC1806 and MCF-7 cells. Nonetheless, taking into account the morphological changes associated with *EXO-DOXO* treatment in these cells, autophagy may not contribute to the distinctive aggressive characteristics of breast cancer.

The *STAT3* signaling pathway can regulate autophagy in different ways, either positively or negatively, depending on the specific cell lines and the phosphorylation sites of *STAT3* [53]. However, in this study, the effect of exosome treatment on InST-BC cells was primarily influenced by the breast cancer subtype. In InST-TNBC cells, the results of exosome treatment indicated the slowing or inhibition of autophagic flux. In contrast, in InST-NTNBC cells, the results of exosome treatment indicated the promoted autophagic flux. Considering the morphological changes observed in breast cancer cells, It can be argued that the aggressive behavior of TNBC, enhanced by exosome treatment, may be dependent on autophagy, whereas that of NTNBC is independent of autophagy.

In this study, compared with treated cells with DOXO without inhibition, DOXO treatment of InST-MDA-MB-231 cells suggested a reduction or blockade of autophagic flux. In contrast, DOXO had no observable effect on autophagic flux in InST-HCC1806 cells, whereas in InST-MCF-7 cells, DOXO treatment appeared to enhance autophagic flux.

The biochemical results of InST-TNBC and InST-NTNBC cells with *EXO-DOXO* treatment compared to *EXO-DOXO* treatment alone suggested that the *STAT3* signaling pathway can negatively or positively regulate autophagy through differences in cell lines and/or *STAT3* phosphorylation sites [53, 54]. In comparison to InST-DOXO-treated cells, the findings indicated that exosomes enhance the aggressive phenotype of TNBC cells through autophagy; however, this effect was not observed in NTNBC cells.

In conclusion, this study aimed to elucidate the influence of human TNBC-derived exosomes on both TNBC and NTNBC cells by investigating the modulation of key signaling pathways involved in cell cycle progression and tumorigenesis, with particular attention to those associated with autophagy. The findings revealed that exosomes may play a role in tumorigenic behavior and chemoresistance, especially in TNBC. In this respect, it could be argued that the aggressive behavior of TNBC potentiated by exosome treatment could be autophagy-dependent, while that of NTNBC is autophagy-independent.

## Author Contribution Statement

S.A.M.A. worked out approximately all of the biotechnical experiments, numerical analysis, and also shared in experiment discussions, and wrote the manuscript with M.A. A. M.A.A. devised the project, the main conceptual ideas, and the proof outline. T.M. I.B., and F.A.O. performed all of the biotechnical details. M.S. worked out the microscopic details for the suggested experiment. Y.M.K. worked out the clinical investigations for the suggested experiment. A.M.H. shared in the experiment and writing the manuscript.

## Acknowledgements

All authors show approval to the Science Technology & Innovation Funding Authority (STDF) for supporting.

*Ethics approval*

A signed informed consent was obtained from each participant in this study in accordance to the rules of Ethics Committee, Medical Research Institute, Alexandria University.

*Availability of data and material*

The data that support the results of this study are available from the corresponding author upon reasonable ask for.

*Funding*

The work was supported by Science Technology &

Innovation Funding Authority (STDF) under grant number [STDF-BARG: (ID: 38145)].

*Competing interests*

The authors declare that there are no conflicts of interest.

*Abbreviations*

Alix: ALG-2-interacting protein-X; ATG16L: autophagy related 16 like 1; ATG5: Autophagy related 5; CD63: cluster of differentiation 63; DMEM: Dulbecco's modified Eagle's medium; DMSO: dimethyl sulfoxide; DOXO: Doxorubicin; ELISA : enzyme-linked immunosorbent assay; EMT: epithelial-mesenchymal transition; ER: estrogen receptor; EXO: Exosomes; Fetal bovine serum : FBS; Her2 protein: human epidermal growth factor receptor 2; IC50: Half-maximal inhibitory concentration; InST cells: Inhibited STAT3 signaling cells; LC3B/ MAP1LC3B: microtubule associated protein 1 light chain 3 beta; MTT: 3-[4,5-dimethylthiazol-2-yl]-2,5 diphenyl tetrazolium bromide; NTNBC : Non- Triple negative breast cancer; PI: Propidium iodide; PR : progesterone receptor; PR: Progesterone Receptor; qRT-PCR: Quantitative real time polymerase chain reaction; RAB24 : Member RAS Oncogene Family 24; ROS: reactive oxygen species; STAT3: signal transducer and activator of transcription 3; TNBC : Triple negative breast cancer; TSG101: tumor susceptibility gene-101; Un-InST cells: uninhabited STAT3 signaling cells.

## References

1. Anders CK, Abramson V, Tan T, Dent R. The evolution of triple-negative breast cancer: From biology to novel therapeutics. Am Soc Clin Oncol Educ Book. 2016;35:34-42. https://doi.org/10.1200/edbk_159135.
2. Yin L, Duan JJ, Bian XW, Yu SC. Triple-negative breast cancer molecular subtyping and treatment progress. Breast Cancer Res. 2020;22(1):61. https://doi.org/10.1186/s13058-020-01296-5.
3. Abd El-Aziz YS, Gillson J, Jansson PJ, Sahni S. Autophagy: A promising target for triple negative breast cancers. Pharmacol Res. 2022;175:106006. https://doi.org/10.1016/j.phrs.2021.106006.
4. You L, Wang Z, Li H, Shou J, Jing Z, Xie J, et al. The role of *STAT3* in autophagy. Autophagy. 2015;11(5):729-39. https://doi.org/10.1080/15548627.2015.1017192.
5. Li X, He S, Ma B. Autophagy and autophagy-related proteins in cancer. Mol Cancer. 2020;19(1):12. https://doi.org/10.1186/s12943-020-1138-4.
6. Qin JJ, Yan L, Zhang J, Zhang WD. *STAT3* as a potential therapeutic target in triple negative breast cancer: A systematic review. J Exp Clin Cancer Res. 2019;38(1):195. https://doi.org/10.1186/s13046-019-1206-z.
7. Donoso-Quezada J, Ayala-Mar S, González-Valdez J. The role of lipids in exosome biology and intercellular communication: Function, analytics and applications. Traffic. 2021;22(7):204-20. https://doi.org/10.1111/tra.12803.
8. Dai J, Su Y, Zhong S, Cong L, Liu B, Yang J, et al. Exosomes: Key players in cancer and potential therapeutic strategy. Signal Transduct Target Ther. 2020;5(1):145. https://doi.org/10.1038/s41392-020-00261-0.
9. Mohamed SA, Badawy TMI, Hussein M, Salama M, El Kerm YM, Mohsen MAA. The involvement of exosomes in the tumorigenicity of breast cancer cell lines through the crosstalk between *STAT3*, notch, and wnt signaling pathways. Discov Oncol. 2025;16(1):1685. https://doi.org/10.1007/s12672-025-03334-0.
10. Jurgielewicz BJ, Yao Y, Stice SL. Kinetics and specificity of HEK293T extracellular vesicle uptake using imaging flow cytometry. Nanoscale Res Lett. 2020;15(1):170. https://doi.org/10.1186/s11671-020-03399-6.
11. Kao J, Salari K, Bocanegra M, Choi YL, Girard L, Gandhi J, et al. Molecular profiling of breast cancer cell lines defines relevant tumor models and provides a resource for cancer gene discovery. PLoS One. 2009;4(7):e6146. https://doi.org/10.1371/journal.pone.0006146.
12. Montcourrier P, Silver I, Farnoud R, Bird I, Rochefort H. Breast cancer cells have a high capacity to acidify extracellular milieu by a dual mechanism. Clin Exp Metastasis. 1997;15(4):382-92. https://doi.org/10.1023/a:1018446104071.
13. Parolini I, Federici C, Raggi C, Lugini L, Palleschi S, De Milito A, et al. Microenvironmental PH is a key factor for exosome traffic in tumor cells. J Biol Chem. 2009;284(49):34211-22. https://doi.org/10.1074/jbc.M109.041152.
14. McCready J, Sims JD, Chan D, Jay DG. Secretion of extracellular HSP90α via exosomes increases cancer cell motility: A role for plasminogen activation. BMC Cancer. 2010;10:294. https://doi.org/10.1186/1471-2407-10-294.
15. Senigagliesi B, Samperi G, Cefarin N, Gneo L, Petrosino S, Apollonio M, et al. Triple negative breast cancer-derived small extracellular vesicles as modulator of biomechanics in target cells. Nanomedicine. 2022;44:102582. https://doi.org/10.1016/j.nano.2022.102582.
16. Shtam T, Naryzhny S, Samsonov R, Karasik D, Mizgirev I, Kopylov A, et al. Plasma exosomes stimulate breast cancer metastasis through surface interactions and activation of FAK signaling. Breast Cancer Res Treat. 2019;174(1):129-41. https://doi.org/10.1007/s10549-018-5043-0.
17. Tang ZH, Li T, Gao HW, Sun W, Chen XP, Wang YT, et al. Platycodin D from Platycodonis Radix enhances the anti-proliferative effects of doxorubicin on breast cancer MCF-7 and MDA-MB-231 cells. Chin Med. 2014;9:16. https://doi.org/10.1186/1749-8546-9-16.
18. Volk-Draper LD, Rajput S, Hall KL, Wilber A, Ran S. Novel model for basaloid triple-negative breast cancer: Behavior in vivo and response to therapy. Neoplasia. 2012;14(10):926-42. https://doi.org/10.1593/neo.12956.
19. Wang X, Pei X, Guo G, Qian X, Dou D, Zhang Z, et al. Exosome-mediated transfer of long noncoding RNA H19 induces doxorubicin resistance in breast cancer. J Cell Physiol. 2020;235(10):6896-904. https://doi.org/10.1002/jcp.29585.
20. Gariboldi MB, Ravizza R, Molteni R, Osella D, Gabano E, Monti E. Inhibition of *STAT3* increases doxorubicin sensitivity in a human metastatic breast cancer cell line. Cancer Lett. 2007;258(2):181-8. https://doi.org/10.1016/j.canlet.2007.08.019.
21. Seguin L, Desgrosellier JS, Weis SM, Cheresh DA. Integrins and cancer: Regulators of cancer stemness, metastasis, and drug resistance. Trends Cell Biol. 2015;25(4):234-40. https://doi.org/10.1016/j.tcb.2014.12.006.
22. Matson JP, Cook JG. Cell cycle proliferation decisions: The impact of single cell analyses. FEBS J. 2017;284(3):362-75. https://doi.org/10.1111/febs.13898.
23. Vakkila J, Lotze MT. Inflammation and necrosis promote tumour growth. Nat Rev Immunol. 2004;4(8):641-8. https://doi.org/10.1038/nri1415.
24. Chen YC, Statt S, Wu R, Chang HT, Liao JW, Wang CN, et al. High mobility group box 1-induced epithelial

mesenchymal transition in human airway epithelial cells. Sci Rep. 2016;6:18815. https://doi.org/10.1038/srep18815.
25. Li M, Liao L, Tian W. Extracellular vesicles derived from apoptotic cells: An essential link between death and regeneration. Front Cell Dev Biol. 2020;8:573511. https://doi.org/10.3389/fcell.2020.573511.
26. Liu Q, Cao Y, Zhou P, Gui S, Wu X, Xia Y, et al. Panduratin A inhibits cell proliferation by inducing G0/G1 phase cell cycle arrest and induces apoptosis in breast cancer cells. Biomol Ther (Seoul). 2018;26(3):328-34. https://doi.org/10.4062/biomolther.2017.042.
27. Poyton RO, Ball KA, Castello PR. Mitochondrial generation of free radicals and hypoxic signaling. Trends Endocrinol Metab. 2009 Sep 1;20(7):332-40.
28. Szmit E, Trzonkowski P, Myśliwska J, Foerster J, Myśliwski A. Ex vivo apoptotic potential of peripheral blood mononuclear cells of the elderly human subject. Cell Biol Int. 2002 Jun 1;26(6):517-27.
29. Alkhalaf M, El-Mowafy AM. Overexpression of wild-type *p53* gene renders MCF-7 breast cancer cells more sensitive to the antiproliferative effect of progesterone. J Endocrinol. 2003;179(1):55-62. https://doi.org/10.1677/joe.0.1790055.
30. Hui L, Zheng Y, Yan Y, Bargonetti J, Foster DA. Mutant p53 in MDA-MB-231 breast cancer cells is stabilized by elevated phospholipase D activity and contributes to survival signals generated by phospholipase d. Oncogene. 2006;25(55):7305-10. https://doi.org/10.1038/sj.onc.1209735.
31. Yang K, Hitomi M, Stacey D. Variations in cyclin D1 levels through the cell cycle determine the proliferative fate of a cell. Cell Div. 2006;1:32. https://doi.org/10.1186/1747-1028-1-32.
32. Weaver JW, Zhang J, Rojas J, Musich PR, Yao Z, Jiang Y. The application of exosomes in the treatment of triple-negative breast cancer. Front Mol Biosci. 2022;9:1022725. https://doi.org/10.3389/fmolb.2022.1022725.
33. Chen HF. Effect of Janus kinase inhibition on extracellular signal-regulated protein kinase during invasion and metastasis of human breast cancer cell MDA-MB-231. Acad J Second Mil Med Univ. 2010:900-3.
34. Sancho-Albero M, Navascués N, Mendoza G, Sebastián V, Arruebo M, Martín-Duque P, et al. Exosome origin determines cell targeting and the transfer of therapeutic nanoparticles towards target cells. J Nanobiotechnology. 2019;17(1):16. https://doi.org/10.1186/s12951-018-0437-z.
35. Nedeljković M, Damjanović A. Mechanisms of chemotherapy resistance in triple-negative breast cancer-how we can rise to the challenge. Cells. 2019;8(9). https://doi.org/10.3390/cells8090957.
36. Khanna P, Lee J, Sereemaspun A, Lee H, Baeg G. GRAMD1B regulates cell migration in breast cancer cells through JAK/STAT and AKT signaling. Sci Rep. 2018;8. https://doi.org/10.1038/s41598-018-27864-6.
37. Burke WM, Jin X, Lin HJ, Huang M, Liu R, Reynolds RK, et al. Inhibition of constitutively active *STAT3* suppresses growth of human ovarian and breast cancer cells. Oncogene. 2001;20(55):7925-34. https://doi.org/10.1038/sj.onc.1204990.
38. Dent R, Trudeau M, Pritchard KI, Hanna WM, Kahn HK, Sawka CA, et al. Triple-negative breast cancer: Clinical features and patterns of recurrence. Clin Cancer Res. 2007;13(15 Pt 1):4429-34. https://doi.org/10.1158/1078-0432.Ccr-06-3045.
39. Lin KL, Su JC, Chien CM, Chuang PW, Chang LS, Lin SR. Down-regulation of the JAK2/PI3K-mediated signaling activation is involved in Taiwan cobra cardiotoxin III-induced apoptosis of human breast MDA-MB-231 cancer cells. Toxicon. 2010;55(7):1263-73. https://doi.org/10.1016/j.toxicon.2010.01.017.
40. Dutta S, Warshall C, Bandyopadhyay C, Dutta D, Chandran B. Interactions between exosomes from breast cancer cells and primary mammary epithelial cells leads to generation of reactive oxygen species which induce DNA damage response, stabilization of p53 and autophagy in epithelial cells. PLoS One. 2014;9(5):e97580. https://doi.org/10.1371/journal.pone.0097580.
41. You L, Mao L, Wei J, Jin S, Yang C, Liu H, et al. The crosstalk between autophagic and endo-/exosomal pathways in antigen processing for MHC presentation in anticancer T-cell immune responses. J Hematol Oncol. 2017;10(1):165. https://doi.org/10.1186/s13045-017-0534-8.
42. Wang ZH, Peng ZL, Duan ZL, Liu H. Expression and clinical significance of autophagy gene Beclin 1 in cervical squamous cell carcinoma. Sichuan da xue xue bao. Yi xue ban=. 2006 Nov 1;37(6):860-3.
43. Pierdominici M, Vomero M, Barbati C, Colasanti T, Maselli A, Vacirca D, et al. Role of autophagy in immunity and autoimmunity, with a special focus on systemic lupus erythematosus. FASEB J. 2012;26(4):1400-12. https://doi.org/10.1096/fj.11-194175.
44. Ylä-Anttila P, Eskelinen EL. Roles for *RAB24* in autophagy and disease. Small GTPases. 2018;9(1-2):57-65. https://doi.org/10.1080/21541248.2017.1317699.
45. Li X, Yan J, Wang L, Xiao F, Yang Y, Guo X, et al. *Beclin 1* inhibition promotes autophagy and decreases gemcitabine-induced apoptosis in MiaPaCa2 pancreatic cancer cells. Cancer Cell Int. 2013;13(1):26. https://doi.org/10.1186/1475-2867-13-26.
46. Yang YP, Hu LF, Zheng HF, Mao CJ, Hu WD, Xiong KP, et al. Application and interpretation of current autophagy inhibitors and activators. Acta Pharmacol Sin. 2013;34(5):625-35. https://doi.org/10.1038/aps.2013.5.
47. Klionsky DJ. Autophagy: From phenomenology to molecular understanding in less than a decade. Nat Rev Mol Cell Biol. 2007;8(11):931-7. https://doi.org/10.1038/nrm2245.
48. Boya P, González-Polo RA, Casares N, Perfettini JL, Dessen P, Larochette N, et al. Inhibition of macroautophagy triggers apoptosis. Mol Cell Biol. 2005;25(3):1025-40. https://doi.org/10.1128/mcb.25.3.1025-1040.2005.
49. Sui X, Chen R, Wang Z, Huang Z, Kong N, Zhang M, et al. Autophagy and chemotherapy resistance: A promising therapeutic target for cancer treatment. Cell Death Dis. 2013;4(10):e838. https://doi.org/10.1038/cddis.2013.350.
50. Vu M, Kassouf N, Ofili R, Lund T, Bell C, Appiah S. Doxorubicin selectively induces apoptosis through the inhibition of a novel isoform of BCL-2 in acute myeloid leukaemia MOLM-13 cells with reduced beclin 1 expression. Int J Oncol. 2020;57(1):113-21. https://doi.org/10.3892/ijo.2020.5052.
51. Garbar C, Mascaux C, Giustiniani J, Merrouche Y, Bensussan A. Chemotherapy treatment induces an increase of autophagy in the luminal breast cancer cell MCF7, but not in the triple-negative MDA-MB-231. Sci Rep. 2017;7. https://doi.org/10.1038/s41598-017-07489-x.
52. Rogov V, Dötsch V, Johansen T, Kirkin V. Interactions between autophagy receptors and ubiquitin-like proteins form the molecular basis for selective autophagy. Mol Cell. 2014;53(2):167-78. https://doi.org/10.1016/j.molcel.2013.12.014.
53. Qu X, Yu J, Bhagat G, Furuya N, Hibshoosh H, Troxel A, et al. Promotion of tumorigenesis by heterozygous disruption of the beclin 1 autophagy gene. J Clin Invest. 2003;112(12):1809-20. https://doi.org/10.1172/jci20039.
54. Xu J, Zhang J, Mao QF, Wu J, Wang Y. The interaction between autophagy and *JAK/STAT3* signaling pathway

in tumors. Front Genet. 2022;13:880359. https://doi.org/10.3389/fgene.2022.880359.